

Determination of effective acceleration voltages in cyclotrons using the phase compression-phase expansion effect

S. Adam, J. Cherix, W. Joho, M. Olivo

S.I.N. - Swiss Institute for Nuclear Research, 5234 Villigen, Switzerland

Summary

A radial voltage distribution of the RF acceleration system in cyclotrons produces a time varying magnetic field. This field compresses the bunch size of the circulating beam for a radially increasing voltage or expands it for a radially decreasing voltage. This phase compression-phase expansion effect was first verified experimentally at the SIN 590 MeV ring cyclotron. The effect can in turn be used to determine the radial voltage distribution very accurately. This method works best for cyclotrons with external ion sources. Measuring the phase history of the beam at the SIN cyclotron with internal phase probes to an accuracy of 10 ps or 0.2° in RF phase allowed a determination of the voltage distribution to an accuracy of about 1 %. Details of the SIN phase measurement system are described.

1. Introduction

The phase compression-phase expansion effect was first mentioned by Mueller and Mahrt<sup>1</sup> and generalized in ref. 2. For an ideal isochronous cyclotron the effect can be described by the following law for the phase history  $\phi(E)$  of a particle at energy E.

$$E_G(E) \times \sin \phi(E) = \text{constant} \quad (1)$$

where  $E_G(E)$  is the peak energy gain per turn. Fig. 1 shows a schematic illustration of the phase compression mechanism coming from the RF magnetic field of the accelerating system. This effect plays an essential role in the second stage of the Indiana cyclotron and in the injector II under construction at SIN. The energy gain in these cyclotrons increases by a factor of 4 and 2.5, respectively, between injection and extraction, corresponding to a phase compression by the same factor. Equation (1) is valid in general; it does not matter if the change in the energy gain comes from a radial variation of the peak voltage or from a change in the transit time factor. The latter effect is clearly seen in the center of a cyclotron, where strong bunching occurs on the first turn after the ion source. Due to the strong curvature of the orbit in the dee gap alternating radial kicks from the electric field produce the bunching.

Contrary to the statements in ref. 1 a tilt of the accelerating gap with respect to the orbits is irrelevant, since the revolution time is not altered by this tilt. This can be proved under the following conditions:

- the focussing frequency  $\nu_r$  and  $E_G$  vary only slowly with radius (adiabaticity condition)
- the coupling between betatron amplitude and phase is taken into account for non-centered orbits.

The proof makes use of the so called symplectic conditions<sup>3</sup> for the elements of the transfer matrix R:

$$\begin{pmatrix} R_{51} \\ R_{52} \end{pmatrix} = \begin{pmatrix} R_{21} & -R_{11} \\ R_{22} & -R_{12} \end{pmatrix} \begin{pmatrix} R_{16} \\ R_{26} \end{pmatrix} \quad (2)$$

The phase compression-phase expansion effect has to be considered in calculating the influence of trim coils. A phase displacement produced by a trim coil at small radii gets damped towards larger radii, if for example the energy gain per turn increases with radius.

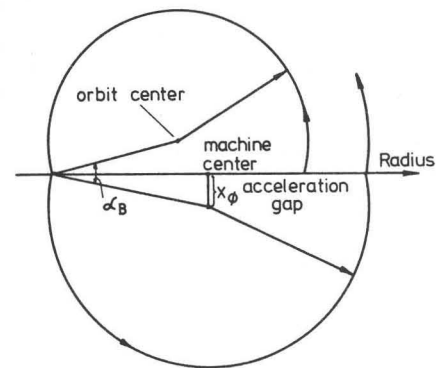


*Fig. 1 Schematic illustration of the phase compression effect. Assumed is a uniform external magnetic field and a 180° dee with radially increasing peak voltage. A particle arriving early (phase  $\phi < 0$ ) at the acceleration gap sees a time dependent magnetic field which gives it a radial outward kick  $\alpha_B$ . Through the resulting longer orbit the particle arrives at the next gap a bit later and moves closer to the central particle with phase 0.*

2. Verification of phase compression at SIN

With the help of phase measurements in the ring cyclotron it was possible to verify equation (1) in 1976 and the results were published in ref. 4. Fig. 2 shows the geometry of an ideal SIN cavity with a cosine-like voltage variation in the radial direction. Fig 3 illustrates the corresponding phase history for 5 reference particles. One clearly sees that the phase width of a beam is first compressed until the maximum energy gain is reached, at a radius of 3.5 m. Towards extraction, at radius 4.5 m, the bunch length expands again slightly. This change in phase width is very difficult to measure directly for a beam which has a typical width of only 6°. The following simple trick was used to avoid this difficulty. The whole beam was shifted in phase prior to injection and the phase history of this displaced beam was then measured and compared with the original phase history. Before discussing the results of these measurements the technique used for measuring phases in the ring is first explained.

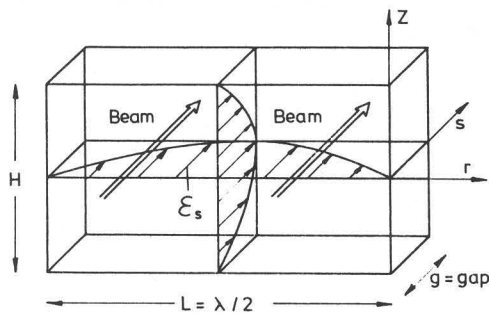


Fig. 2 Geometry of a rectangular  $\lambda/2$  cavity (SIN cavity operating in the  $H_{101}$ -mode). There is only an electric field component  $\epsilon_s$  with a sinusoidal distribution in the  $r$ - and  $z$ -direction. The RF magnetic field is confined in the  $(r,z)$ -plane, and the beam passes through the cavity in the  $s$ -direction.

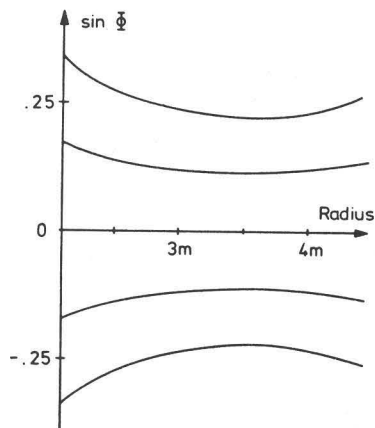


Fig. 3 Phase history of 5 reference particles in the ideally isochronized ring cyclotron. The cosine-like distribution of the peak cavity voltage leads to a compression and later to an expansion of the bunch size. For each particle the relation "energy gain  $\times$   $\sin \phi = \text{constant}$ " holds.

### 3. Experimental Setup

The proton bunches in the circulating beam induce a signal on a non-intercepting pair of  $50 \Omega$  terminated capacitive pick-up plates. A schematic of the phase probe built into the SIN ring cyclotron<sup>5</sup> is shown in fig. 4. There are 11 pairs of identical pick-up plates positioned at fixed radii. The copper electrodes are rectangular in shape 50 mm radially  $\times$  25 mm azimuthally. They are located above and below the median plane, 40 mm apart. The pick-up plates are mounted inside an aluminum frame, the whole structure forming a  $50 \Omega$  micro-strip line.

The functional diagram of the phase probe electronics is shown in fig. 5. A sampling method is used to detect the beam induced signals. The signals from the upper and lower plates are summed at the cyclotron vacuum wall and sent to the sampling units. Because the four 50 MHz accelerating cavities, each operating at a peak voltage of 500 kV, make the ring bunker "rich" in RF noise, the sampling units were installed away from this environment. Furthermore, special care was taken in the

choice of the coaxial cables used to transport the weak signals ( $370 \mu\text{V}/\mu\text{A}$  for the innermost pick-up plates). Fig. 6 shows the calculated effect of two different, 40 m long, coaxial cables on the shape of the expected signal as compared to a lossless cable. The chosen coaxial cable, Cellflex 1/2", has a solid outer shielding and an attenuation of 2.4 dB/100 m at 100 MHz.

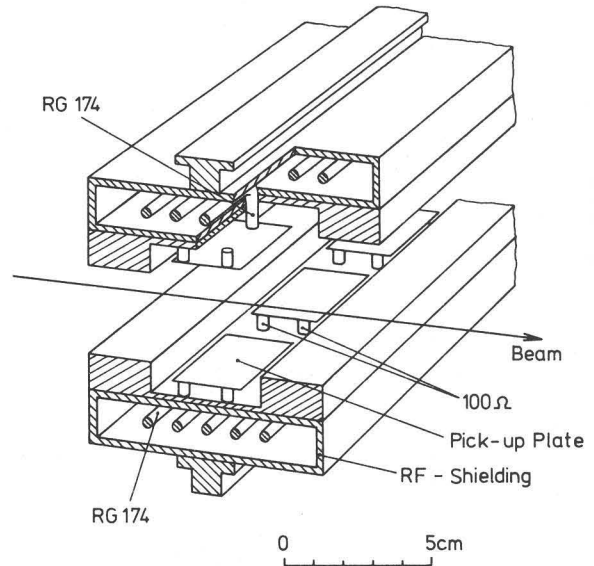


Fig. 4 A cut-away drawing of phase probe. The copper pick-up plates (25 mm  $\times$  50 mm) together with the aluminum support structure form a  $50 \Omega$  micro-strip line. The pick-up plates are embedded into the support structure in order to reduce the 50 MHz noise arising from the RF field leaking out of the ring accelerating cavities. The upper and lower plates are 40 mm apart.

In order to reduce the still remaining RF pick-up noise a test was carried out using the "odd-sampling" technique<sup>6</sup>. This method brought however no significant improvement, the reason being that a good portion of the RF noise appears to come from the four 50 MHz 125 kW power amplifiers which are installed close to the cavities. These amplifiers produce higher harmonics and only the odd ones are filtered out by the "odd-sampling" technique. As a result the even harmonics remain while the amplitude of the beam induced signal is reduced by a factor of 2.

Because the coaxial cables built into the ring vacuum chamber (RG 174) are of different length, the difference in the time of flight is electronically compensated in the sampling units. A reference signal, from the master oscillator, is also sampled. The resulting low frequency signals are sent to the control room where they are amplified. An automatic gain control unit ensures a constant signal output for a beam intensity variation from 2  $\mu\text{A}$  (set-up of the ring machine) to the highest achieved level of 110  $\mu\text{A}$ . A sweeper with a repetition frequency of 1.3 Hz is used to ramp the driver as well as the storage scope. The driver itself



generates the trigger pulses (1 out of 64 RF cycles) for the sampling units. A filter with a cut-off frequency of 33 Hz is used to block the 50 Hz line frequency noise. The phase signals, together with the reference, are displayed via a multiplexer on a storage scope. Each phase signal is sent also to the zero-cross-over units, which generate the start pulse for the counters. The counters are subsequently stopped by the reference signal. The phase values are digitally displayed or read directly by the computer

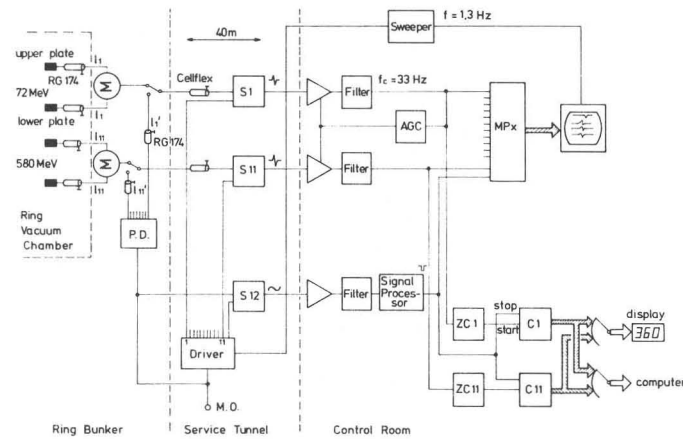


Fig. 5 Block diagram of the phase probe electronics.

The summed upper and lower beam induced signals are sent through a 40 m long Cellflex cable to the sampling units. The signal from the master oscillator (M.O.), which provides the reference frequency to the cyclotron's RF accelerating systems, is delivered to the eleven sampling units ( $S_{1-11}$ ) and to the power divider (P.D.). The sampling unit  $S_{12}$  generates the stop signal for the counters  $C_{1-11}$  as well as the reference signal for display in the storage scope.

Calibration of the electronics is done by switching units  $S_{1-11}$  to the reference signals delivered by the power divider. The RG 174 power divider cables ( $l'_{1-11}$ ) are correspondingly equal in length to the RG 174 phase probe cables ( $l_{1-11}$ ).

An automatic gain control unit (AGC) adjusts the gain of the eleven amplifiers to ensure a beam intensity independent signal for the zero-cross-over units, which generate the start signal for the counters.

An RF signal from the master oscillator is sent, through a power divider and an equivalent set of RG 174 cables ( $l'_{1-11}$ ), to the sampling units (via eleven remote controlled coaxial switches) for calibration purposes. The sampling units are, for routine operation, adjusted monthly to  $\pm 0.4^\circ$ , the drift being  $< + 1^\circ$  in that period. A change in the beam induced signal duty cycle from 5% to 2.5% results in the following phase shifts:  $0.36^\circ$  due to the 40 m long Cellflex cable,  $0.09^\circ$  due to the RG 174 cable and  $0.63^\circ$  due to the 33 Hz filter. A change in the cut-off frequency of this filter by 1.3 Hz results in a phase shift of  $0.17^\circ$ .

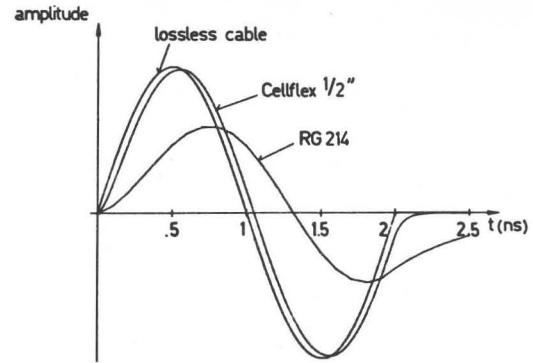


Fig. 6 Calculated phase shift and amplitude change for two different cables (Cellflex  $\frac{1}{2}$ " and RG 214) as compared with a lossless cable. The magnitude of these changes are a function of the beam duty cycle.

Computer processed phase probe signals are shown in fig. 7 for an internal beam intensity of  $8 \mu A$ . The raw signals from the phase probe are shown in fig. 8 for a  $6 \mu A$  beam with a purposely de-tuned magnetic field. The beam coming back was stopped on an internal radial probe to protect the Ring Electrostatic In-flector Channel (EIC).

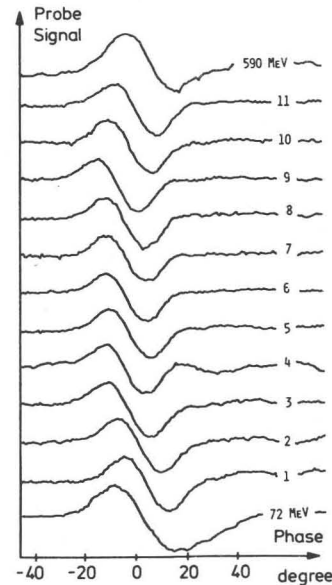


Fig. 7 Phase probe signals from an  $8 \mu A$  circulating beam in ring cyclotron. Displayed are the signals from 11 internal capacitive phase probes as well as from two external probes before injection (72 MeV) and after extraction (590 MeV). Digital filters were used to reject high frequency noise and to smooth out statistical errors. The figure shows the probe signals after digital processing. Time (or phase) increases towards the right.

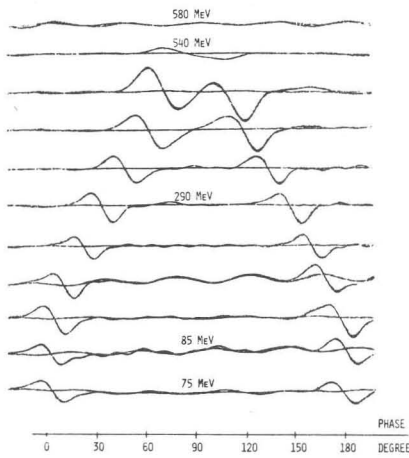


Fig. 8 Eleven phase probe signals from accelerated and decelerated beam in the ring cyclotron. For this experiment the current of the main magnet was lowered by 0.06%. The particle bunches injected into the ring at 0° slipped out of phase with the RF system close to extraction (phase = 90°). They were then decelerated back towards the injection energy (phase = 180°). To see clearly the effect of the circulating particles the beam was shut off for a short moment, leading to the approximately constant background signal.

#### 4. Measurement of radial voltage variation

The RF electric fields are normally difficult to measure accurately. The phase compression - phase expansion effect gives us the possibility of converting this problem into an easier one of measuring time intervals. We determine the radial variation of the energy gain per turn through a measurement of different phase histories. By counting the total number of turns in the cyclotron we obtain an absolute calibration for the average energy gain. The point at which the phase of the beam is zero is obtained by the following two methods, as explained in another paper of this conference<sup>7</sup>:

- maximizing the acceleration of the beam over the first few turns in the ring cyclotron
- tuning the cyclotron for single turn extraction.

For an evaluation of the different phase histories  $\phi(E)$  we have to modify equation (1) slightly. For a cyclotron which is not perfectly isochronous, the Hamiltonian  $H$  for the variable  $E(n)$  and  $\phi(n)$  is given by<sup>2</sup>

$$H(E, \phi) = E_G(E) \sin \phi(E) - \int \phi_{ni}(E) dE \quad (3)$$

where  $n$  is the turn number and  $\phi_{ni}$  the phase shift per turn due to magnetic field errors.

The Hamiltonian  $H$  is a constant of motion. This allows the elimination of the integral in (3) and leads to a quick determination of the energy gain from the phase histories  $\sin \phi(E)$ . The result of this procedure is shown in fig. 9. The radial variation of the energy gain was measured with an accuracy of about 1%. The agreement with the predicted curve

for an ideal SIN cavity is rather good. The deviations at injection are believed to come from the asymmetric lips inside the cavity. These lips were installed in order to minimize transit time effects which are of the order of 1% at injection.

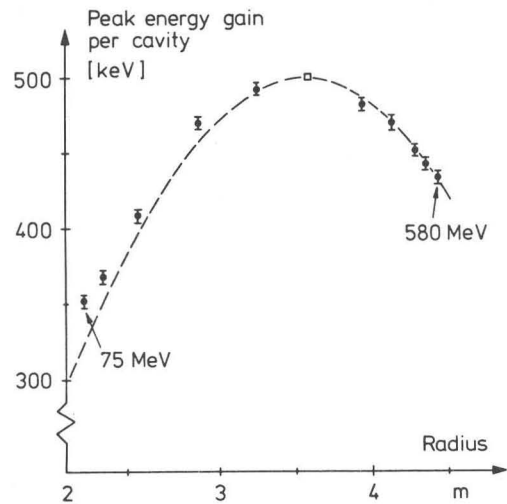


Fig. 9 The radial distribution of the peak energy gain per turn for the SIN cavities. The dots represent measured values with respect to the reference value marked with a little square. The broken line corresponds to a pure cosine distribution for an ideal rectangular cavity. Absolute calibration of the cavity voltage is performed by counting the total number of turns in the cyclotron.

#### References

1. R.W. Mueller and R.W. Mahrt, Nucl. Instr. and Meth. 86 (1970) 24
2. W. Joho, Particle Accelerators, 6 (1974) 41
3. G. Hinderer, VICKSI Berlin, Thesis Jan. 1975
4. W. Joho, M. Olivo, T. Stambach, H. Willax, Particle Acc. Conf. 77, IEEE Trans. Nucl. Sci., NS-24, No 3, 1618 (1977)
5. M. Olivo, Proc. 7th Int. Conf. on Cyclotrons and their Applications (Birkhäuser, Basel, (1975), 331
6. J.F.P. Marchand, F. Schutte, H.L. Hagedoorn, Rev. Sci. Instr. 45 (1974) 361
7. W. Joho, S. Adam Setting up the 590 MeV ring cyclotron for single turn extraction, this conference.

\*\* DISCUSSION \*\*

M. CRADDOCK: How does the accuracy of this method of measuring the energy gain as a function of radius compare with direct measurement of the radius gain between individual turns?

W. JOHO: If you do a careful analysis of the turn pattern, taking care of coherent oscillations and the phase history, you can get about 1% accuracy as well. However, we did not have time to do this through the entire range of the cyclotron.